



## Research article

# DNMT3A-mediated DNA methylation and transcription inhibition of FZD5 suppresses lung carcinogenesis

Jiqiao Shen <sup>a</sup>, Jinchen Su <sup>b</sup>, Xiangling Chu <sup>c</sup>, Xin Yu <sup>c</sup>, Xiwen Gao <sup>a,\*</sup>

<sup>a</sup> Department of Respiratory and Critical Care Medicine, Minhang Hospital, Fudan University, Shanghai, 201100, China

<sup>b</sup> School of Medicine, Shihezi University, Shihezi, 832000, Xinjiang, China

<sup>c</sup> Department of Oncology, Shanghai Pulmonary Hospital, Tongji University School of Medicine, Shanghai, 200000, China

## ARTICLE INFO

## Keywords:

Urethane

NSCLC

FZD5

DNMT3A

## ABSTRACT

**Background:** Based on the bioinformatics prediction, this study investigates the correlation between aberrant transcription factor Frizzled 5 (FZD5) expression and the establishment of non-small cell lung cancer (NSCLC).

**Methods:** A mouse model with regard to primary NSCLC was encouraged by intraperitoneal injection of urethane. Lentivirus-based FZD5 silencing was then administered to examine its role in tumorigenesis in the mouse lung. Silencing of FZD5 was induced in two NSCLC cell lines to examine its function in the malignant behavior pertaining to cells *in vitro*. Quantitative methylation-specific PCR was employed to assess the DNA methylation level within the NSCLC cells. DNA methyltransferases (DNMTs) that administer FZD5 were assessed by chromatin immunoprecipitation assay. Consequently, overexpression of DNMT3A was introduced in mice and NSCLC cells to verify its regulation on FZD and its biological roles in NSCLC development.

**Results:** In NSCLC, FZD5 expression is elevated, and its knockdown reduced tumor incidence rate in the urethane-challenged mice. The FZD5 silencing also inhibited proliferation, migration, as well as invasion with regard to Calu-3 and NCI-H1299 cells *in vitro*. The aberrant upregulation with regard to FZD5 in NSCLC was due to at least partly by reduced promoter methylation level. DNMT3A, which bound to FZD5 promoter to suppress its transcription, was poorly expressed in NSCLC. Artificial upregulation of DNMT3A suppressed urethane-induced lung carcinogenesis in mice and suppressed the malignant phenotype pertaining to NSCLC cells *in vitro*.

**Conclusion:** This research demonstrates that the lack of DNA methylation level-induced activation of FZD5 is correlated with NSCLC's onset and progression.

## 1. Introduction

Lung cancer, which ranks second in the world in terms of prevalence (11.4%) and is the primary driver of deaths related to cancer (18%) in the year 2020 [1], remains a major global health concern. Lung cancer refers to the most prevalent kind of cancer in China, with the greatest incidence as well as death rates of any cancer [2]. It is commonly known that smoking cigarettes is the main and of greatest significance risk factor for establishing as well as developing lung cancer. Furthermore, studies have determined that secondhand smoke can increase the chance of developing lung cancer by up to 26% [3,4]. Lung squamous cell carcinoma (LUSC) as

\* Corresponding author.

E-mail address: [xiwengao@sina.com](mailto:xiwengao@sina.com) (X. Gao).

<https://doi.org/10.1016/j.heliyon.2024.e29733>

Received 1 January 2024; Received in revised form 9 April 2024; Accepted 15 April 2024

Available online 16 April 2024

2405-8440/© 2024 Published by Elsevier Ltd.

This is an open access article under the CC BY-NC-ND license

(<http://creativecommons.org/licenses/by-nc-nd/4.0/>).

well as lung adenocarcinoma (LUAD) refers to the most prevalent subtypes of non-small cell lung cancer (NSCLC), accounting for about 85 % of newly diagnosed patients [5]. Hence, surgical resection is a highly successful and common treatment for NSCLC in the early stages; patients who are not good candidates for surgery should receive chemotherapy or radiation therapy instead [6,7]. Nevertheless, the prognosis for patients who have advanced lung cancer is frequently dire, making it imperative to find promising biomarkers and create therapeutic targets in order to diagnose patients early and treat them effectively.

In this study, by performing transcriptome analysis using gene expression datasets available from publicly accessible systems, we discovered that a potential gene that may be highly expressed in NSCLC as well as correlated with poor patient outcomes is frizzled class receptor 5 (FZD5). The Wnt/ $\beta$ -catenin signaling pathway, which is greatly conserved as well as serves vital roles in embryonic development, homeostasis, tissue regeneration, as well as oncogenesis, is largely composed of FZD proteins [8]. To date, ten FZD receptor subtypes have been recognized, which play distinct and irreplaceable functions in different biological processes [9]. The versatile effects pertaining to the Wnt/ $\beta$ -catenin signaling pathway could differ based on the specific ligand-receptor interactions, and the FZD receptors partly contribute to the diversity of Wnt signaling responses [10–12]. In a variety of human cancers, including NSCLC, Wnt signaling constitutes a master oncogenic pathway [13]. Yet, the precise expression pattern as well as the role of FZD5 in lung cancer, are still largely unknown.

DNA methylation, a crucial epigenetic process, is the incorporation of a methyl group into cytosine's C5 position, generating 5-methylcytosine in the process [14]. The methyl group is primarily added covalently at cytosine sites in CpG dinucleotides, clustering them together to form large groups called CpG islands [15]. Promoter hypermethylation typically suppresses gene transcription, while hypomethylation leads to gene activation, overexpression, or abnormal expression of transposons [16]. Aberrant DNA methylation patterns contribute to genomic instability, thereby contributing to various disorders, including cancer [17]. Notably, the development as well as advancement of lung cancer are closely linked to irregular DNA methylation patterns [16,18,19]. Particularly, the process of DNA methylation is dynamic as well as reversible, making methylation modifications potential targets for treatment [20]. There exist three common DNA methyltransferases (DNMTs), DNMT1, DNMT3A, as well as DNMT3B, in charge of catalyzing the addition of methyl groups to cytosine residues at Carbon 5, leading to DNA hypermethylation [21]. Thus, this particular research employed two NSCLC cell lines, including urethane-treated mouse models to investigate the roles of FZD5 along with its regulatory DNMT in lung tumorigenesis.

## 2. Materials and methods

### 2.1. Development of a mouse model of primary lung cancer

The Animal Care Committee of Minhang Hospital, Fudan University, approved the guidelines for the use of C57BL/6 mice, which were attained from Vital River Laboratory Animal Technology Co., Ltd. (Beijing, China) (Approval number: 2023-MHFY36JZS). The mice were induced to encounter primary NSCLC by weekly intraperitoneal injections of 1 g/kg urethane (94300, Sigma-Aldrich Chemical Company, Merck KGaA, Darmstadt, German) for a duration of 10 weeks. After two months of urethane administration, artificial gene alteration was induced in the mice through tail vein injection of lentiviral vectors featuring the negative control (NC) plasmids (oe-NC or sh-NC), the overexpression DNMT3A or FZD plasmids (oe-DNMT3A/oe-FZD), or the short hairpin (sh) RNA of FZD5 (each one supplied by the VectorBuilder Inc., Guangzhou, Guangdong, China). These mice were divided into 5 groups total, each containing eight mice: sh-NC, sh-FZD5, oe-NC, oe-DNMT3A, and oe-DNMT3A + oe-FZD5 groups. Four months after the final urethane treatment, by injecting an excessive amount of nembital (140 mg/kg) intraperitoneally, the mice were put down. The lung tissues were then quickly gathered, captured, in addition to the number of tumor nodules was recorded. The lung tissues were then frozen at  $-80^{\circ}\text{C}$  or fixed in paraformaldehyde for subsequent analyses.

### 2.2. Reverse transcription quantitative polymerase chain reaction (RT-qPCR)

Utilizing the TRIzol reagent (Thermo Fisher Scientific, Rockford, IL, USA), RNA derived from tissues or NSCLC cells (see details later) was isolated. A reverse transcription kit (11483188001, Roche Ltd, Basel, Switzerland) was then utilized to convert the extracted RNA to cDNA. Consequently, the TB Green® Fast qPCR Mix (RR430A, Takara Holdings Inc., Kyoto, Japan) was employed to set up and amplify the PCR system. The  $2^{-\Delta\Delta\text{Ct}}$  technique was utilized to detect relative gene expression, having GAPDH serves as the endogenous loading. The primer sequence (all 5'-3') information is given below: mouse FZD5 primer (F) CCAGTGCAAGTCCATTACGGC, (R) CCAAGACAAAGCCTCGTAGTGAG; mouse DNMT3A primer (F) CGCAAAGCCATCTAGGAAGTCC, (R) GCTTGTCTGCACTTCCACAGC; mouse GAPDH primer (F) CATCACTGCCACCCAGAAGACTG, (R) ATGCCAGTGAGCTTCCCGTTCAG; human FZD5 primer (F) TGGAACGCTTCCGCTATCCTGA, (R) GGTCTCGTAGTGATGTGGTTG; human DNMT3A primer (F) CCTCTTCGTTGGAGGAATGTGC, (R) GTTTCGCGACATGAGCACCTCA; and human GAPDH primer (F) GTCTCCTGACTTCAACAGCG, (R) ACCACCTGTTGCTGTAGCCAA.

### 2.3. Hematoxylin and eosin (HE) staining

The lung tissues with regard to the mouse were fixed, paraffined, and cut into segments. Consequently, the segments were subsequently rehydrated, deparaffined, and incubated with hematoxylin for 5 min. The sections were then cleaned, immersed in an HCl/ethanol solution, and allowed to stain for 2 min using an eosin solution. Subsequently, the sections underwent dehydration, were cleared in xylene, as well as sealed to enable microscopic examination.

#### 2.4. Immunohistochemistry (IHC)

In order to facilitate heat-mediated antigen retrieval, the prepared mouse lung tissue sections were first deparaffined, then rehydrated, as well as immersed in EDTA solution. After that, the sections were incubated for a period of 20 min with 3 % H<sub>2</sub>O<sub>2</sub> for 20 min as well as blocked for 30 min with normal goat serum. Afterwards, they were incubated for a period of 16 h at 4 °C having the antibodies of FZD5 (1:200, ab75234, Abcam Inc., Cambridge, MA, USA) as well as PCNA (1:1000, 10205-2-AP, Proteintech Group, Inc., Wuhan, Hubei, China). Correspondingly, the sections were incubated for a period of 30 min at room temperature, having goat anti-rabbit IgG (1:2000, ab205718, Abcam). Here, the sections underwent nuclear staining with hematoxylin and DAB color development, followed by dehydration, xylene clarification, as well as sealing for microscopic examination.

#### 2.5. Cells and lentivirus-based transfection

The American Type Culture Collection (Manassas, VA, USA) provided the human lung fibroblasts CCD-19Lu. Meanwhile, Procell Life Science & Technology Co., Ltd. (Wuhan, Hubei, China) supplied the NSCLC cell lines NCI-H1299 as well as Calu-3. Calu-3 cells were grown in MEM, NCI-H1299 cells in RPMI-1640, as well as CCD-19Lu cells in DMEM/F12K. 10 % fetal bovine saline and 1 % antibiotics were added to all media, and every single cells was cultured with 5 % CO<sub>2</sub> at 37 °C.

The NCI-H1299 as well as Calu-3 cells were given lentiviral vectors-carried sh-FZD5, oe-DNMT3A, oe-FZD, and the corresponding NC plasmids as well for *in vitro* experiments. The appropriate antibiotics were used to screen cells that were transfected and steadily infected.

#### 2.6. Western blot (WB) analysis

For the extraction of total protein, cells were lysed in RIPA lysis buffer on ice. A bicinchoninic acid kit (P0012S, Beyotime Biotechnology Co. Ltd., Shanghai, China) was put to use in order to determine the protein concentration. Subsequently, a protein sample of the same amount was separated via SDS-PAGE and transferred onto polyvinylidene fluoride membranes. Consequently, for 2 h, the membranes were blocked in 5 % non-fat milk. Next, they were probed for a period of 1 h at room temperature using an HRP-conjugated secondary antibody (1:2,000, ab205718, Abcam) and the primary antibodies at 4 °C. The enhanced chemiluminescence reagent (34580, Thermo Fisher Scientific) was put to use to visualize the blot bands. Relative protein level, with GAPDH as the loading control, was determined using the Image J software. Here, the primary antibodies used included FZD5 (1:1000, ab75234, Abcam), DNMT3A (1:1000, 3598, Cell Signaling Technology, Beverly, MA, USA) as well as GAPDH (1:3000, ab9485, Abcam).

#### 2.7. Cell counting kit-8 (CCK-8) method

The treated NCI-H1299 as well as Calu-3 cells were suspended in complete medium, and approximately 2000 cells in a 100 µL cell suspension were incorporated into each well of a 96-well plate. Following the incubation for specific durations (0, 24, 48, 72 h), 10 µL of CCK-8 reagent (C0037, Beyotime) was incorporated into each well and left for an additional hour. To assess the viability of the cells, the optical density at 450 nm was established.

#### 2.8. Colony formation assay

Note that 2000 cells per well of six-well plates were seeded with the treated NCI-H1299 and Calu-3 cells. Following two weeks of cell culture with 5 % CO<sub>2</sub> at 37 °C, the cells were fixed for a period of 15 min with 4 % paraformaldehyde as well as stained for a period of 5 min with crystal violet. Under a microscope, the number with regard to cell colonies was determined.

#### 2.9. Wound-healing assay

In 12-well plates supplemented with serum-free medium, the treated NCI-H1299 and Calu-3 cells were cultured at a density of 5 × 10<sup>5</sup> cells per well. Here, a sterile pipette tip was put to use to create scratches on the cell monolayer once an 80 % confluence had been attained. After rinsing away the cell debris, the wound's width at 0 and 24 h was measured and recorded. Next, the Image J software was utilized to examine the cells' 24-h migration rate.

#### 2.10. Transwell assay

The treated NCI-H1299 as well as Calu-3 cells were resuspended in serum-free medium. They were then put into the 24-well Transwell chambers' upper wells, which were pre-coated with Matrigel. The lower wells were added with a 600 µL medium that included 10 % FBS. The cells that had invaded the lower membranes were fixed as well as stained with crystal violet after a 24-h cell culture at 37 °C and 5 % CO<sub>2</sub>.

#### 2.11. Quantitative methylation specific PCR (qMSP)

A FlexiGene DNA Kit (51206 m, Qiagen GmbH, Hilden, Germany) was the instrument used to extract the cellular DNA. Meanwhile,

EZ DNA Methylation-Lightning Automation Kit (D5049, Zymo Research Corporation, Irvine, CA, USA) was utilized for modifying it with bisulfite. Following that, utilizing the Power SYBR Green PCR Premix (4368708, Applied Biosystems, Inc., Carlsbad, CA, USA), 1  $\mu$ L of the DNA product was used for qMSP analysis. 1.5 % agarose gel electrophoresis was performed on the PCR product, whereas the unmethylated PCR product was utilized as a normalization.

## 2.12. Chromatin immunoprecipitation (ChIP)

The NCI-H1299 as well as Calu-3 cells, were crosslinked at 37 °C in 1 % formaldehyde for a period of 10 min. Consequently, for a period of 5 min, they were quenched with glycine. This aligns with the directions provided by the EZ-Magna ChIP® G ChIP kit (17-409, Sigma-Aldrich, Merck KGaA, Darmstadt, Germany). Correspondingly, the cells were lysed on ice as well as subjected to ultrasonication to produce a chromatin truncation of 200–1000 bp. DNMT1 (1:50, 5032, Cell Signaling Technology, Beverly, MA, USA), DNMT3A (1:50, 3598, Cell Signaling Technology), as well as DNMT3B (1:20, NB300-516, Novus Biologicals) antibodies were then incorporated to the lysates and left overnight at 4 °C. In order to determine the abundance of FZD5 promoter fragments, the protein-chromatin complexes were gathered via magnetic beads and de-crosslinked. Lastly, the DNA was eluted as well as purified for qPCR analysis.

## 2.13. Promoter luciferase reporter assay

After oe-DNMT3A or oe-NC were transfected into NCI-H1299 as well as Calu-3 cells, the FZD5 promoter sequence was incorporated into the pGL3-basic luciferase reporter vector (Promega Corporation, Madison, WI, USA). Utilizing the luciferase detection kit (HY-K1013, MedChem Express, Monmouth Junction, NJ, USA), the luciferase activity in the cells was assessed after a 24-h period.

## 2.14. Statistical analysis

The Prism 8.0 software was utilized for analyzing the data (GraphPad, La Jolla, CA, USA). Every piece of information gathered from three biological replicates, at the very least, is displayed as the mean  $\pm$  standard deviation. When appropriate, the Student's t-test or a one- or two-way Analysis of Variance (ANOVA) was employed to generate a comparison of the distinctions between the groups. Here, statistically significant difference was set at  $p$  less than 0.05.

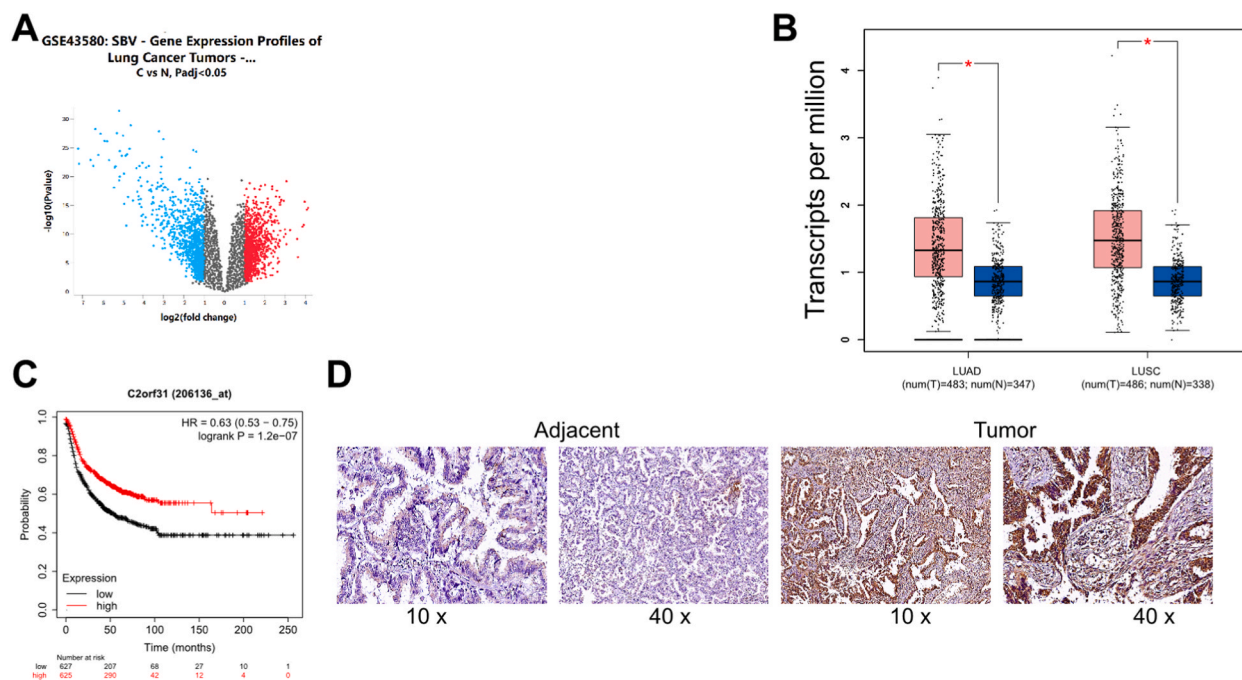


**Fig. 1.** FZD5 is highly expressed in NSCLC and linked to poor prognosis. A, differentially expressed genes between NSCLC samples and control tissue samples in the GSE43580 datasets; B, expression pattern of FZD5 in TCGA-LUAD and TCGA-LUSC systems; C, correlation between KZD expression and the prognosis of patients with LUAD or LUSC in the KM-Plotter database; D, FZD5 expression and in NSCLC tissue microarrays analyzed by IHC.

### 3. Results

#### 3.1. FZD5 is highly expressed in NSCLC and linked to poor prognosis

By assessing the GEO datasets GSE43580, we attained FZD5 as a shared differentially expressed gene that, in NSCLC samples, is highly expressed (refer to Fig. 1A). Furthermore, FZD5 is greatly expressed in LUAD and LUSC samples, per data from the online TCGA database (<https://portal.gdc.cancer.gov/>) (see Fig. 1B). The KMplotter database indicates that patients with NSCLC who have high expression of FZD5 have a worse prognosis (refer to Fig. 1C). Moreover, we employed IHC techniques to evaluate the protein content of FZD5 in tissue microarrays that included tumor tissues as well as adjacent tissues from NSCLC patients obtained from Aifang Bio (China). We discovered that FZD expression was significantly greater in the NSCLC tissues in comparison to the normal tissues (see Fig. 1D).

#### 3.2. Inhibition of FZD5 inhibits urethane-induced lung tumorigenesis in mice

C57BL/6 mice were challenged with urethane to induce lung tumorigenesis, followed by tail vein injection concerning lentiviral vectors-carried sh-NC or sh-FZD5. Indeed, the sh-FZD5 administration reduced FZD5 mRNA expression in the mouse lung tissues after animal sacrifice (Fig. 2A). This led to significantly decreased tumor incidence rate (Fig. 2B) in addition to the number of tumor nodules (Fig. 2C–D). The HE staining showed that the FZD5 silencing significantly ameliorated the pathological changes in the lung tissue, as manifested by enhanced tissue structure and alleviations in the dense cell nucleus proliferation and tumor cell infiltration (Fig. 2E). The IHC assay further showed that the sh-FZD5 administration reduced the positive staining of FZD5 and the proliferation marker PCNA in the mouse lungs (Fig. 2F–G).

#### 3.3. FZD5 silencing alleviates malignant properties of NSCLC cells in vitro

To investigate FZD5's biological role in NSCLC in more detail, lentiviral vectors-carried sh-FZD5 was administered into the NCI-H1299 and Calu-3 cell lines. This successfully led to a decrease in the mRNA (Fig. 3A) as well as protein (Fig. 3B) expression of FZD5 in those cell lines. The cells' abilities to proliferate and form colonies were significantly inhibited in this environment (refer to Fig. 3C–D). Additionally, the Transwell assays in addition to wound healing demonstrated that the migration (see Fig. 3E) as well as invasiveness (Fig. 3F) of the two cell lines were suppressed upon FZD5 silencing as well.

#### 3.4. DNMT3A promotes methylation of the FZD5 promoter

RT-qPCR results indicated that, in comparison to normal CCD-19Lu cells, the NSCLC cell lines NCI-H1299 as well as Calu-3 had significantly higher levels of FZD5 mRNA expression (Fig. 4A). This was at least partially associated with the decreased promoter

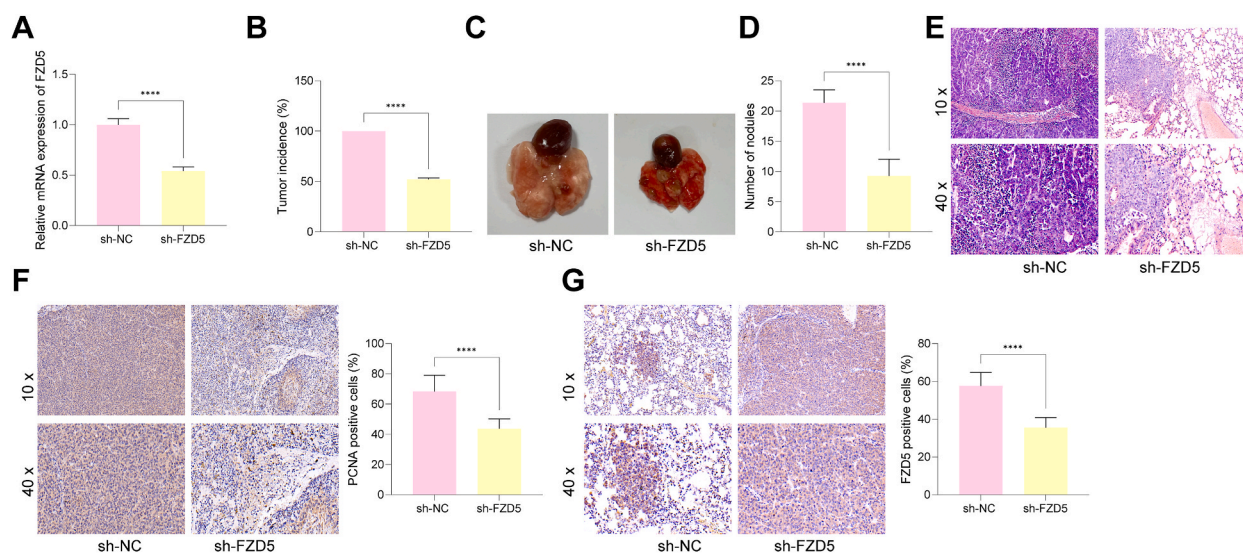


**Fig. 2.** Inhibition of FZD5 inhibits urethane-induced lung tumorigenesis in mice. C57BL/6 mice were challenged with urethane to induce lung tumorigenesis, followed by tail vein injection of lentiviral vectors-carried sh-FZD5 or sh-NC. A, FZD5 mRNA in the mouse lung tissues examined by RT-qPCR (n = 8); B, tumorigenesis rate in the mouse lung (n = 8); C, representative images of the mouse lung in each group; D, number of tumor nodules in the mouse lung (n = 8); E, pathological changes in the mouse lung examined by HE staining; F–G, expression of PCNA (F) and FZD5 (G) in the mouse lung tissues examined by the IHC assay (n = 8). Differences are compared by the unpaired *t*-test. \**p* < 0.05.

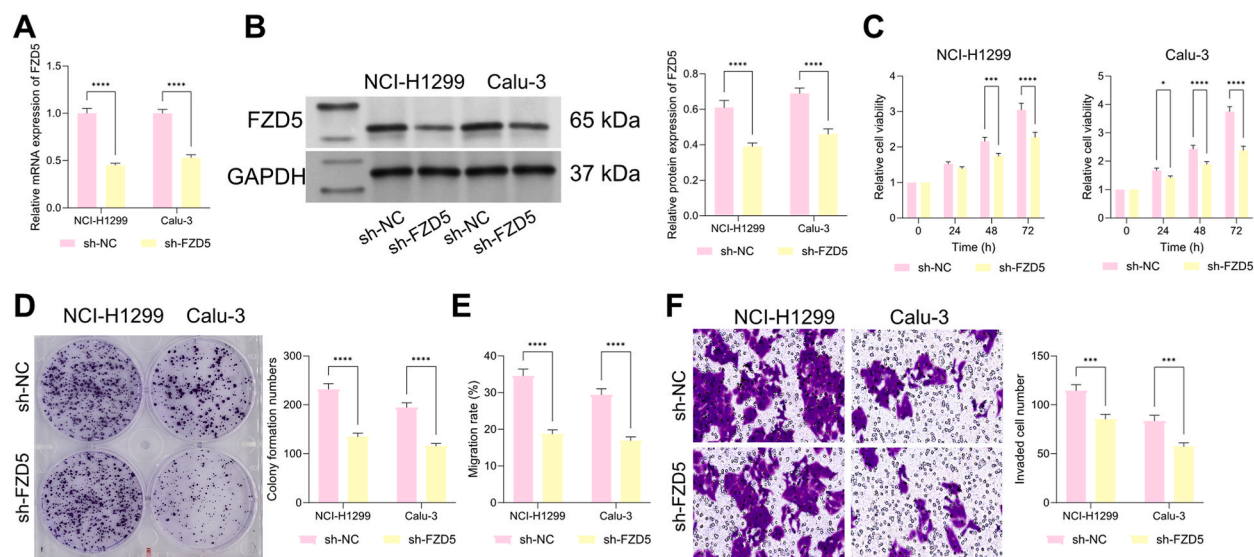


**Fig. 3.** FZD5 silencing alleviates malignant properties of NSCLC cells *in vitro*. sh-FZD5 was administered into the NCI-H1299 and Calu-3 cell lines A-B, mRNA (A) and protein (B) levels of FZD5 in cells determined by RT-qPCR and WB analysis, respectively ( $n = 3$ ); C-D, proliferation (C) and colony formation (D) assay of the NCI-H1299 and Calu-3 cells determined by CCK-8 and colony formation assays, respectively ( $n = 3$ ); E-F, migration (E) and invasion (F) of NCI-H1299 and Calu-3 cells analyzed by wound healing and Transwell assays. Differences are compared by the two-way ANOVA. \* $p < 0.05$ .

methylation level as detected by the qMSP analysis (Fig. 4B). Thereafter, we examined the binding between several DNMTs (DNMT1/DNMT2/DNMT3A/DNMT3B) and FZD5 promoter in NCI-H1299 and Calu-3 cells using ChIP-qPCR assay. Interestingly enough, only DNMT3A as well as the FZD5 promoter were shown to have a direct binding relationship (see Fig. 4C). Moreover, low DNMT3A mRNA as well as protein levels were found in the Calu-3 and NCI-H1299 cells (see Fig. 4D and E). Subsequently, oe-DNMT3A was administered into the two cell lines. DNMT3A expression significantly increased as a result of this (Fig. 4F), along with a downregulation of the FZD5 mRNA (Fig. 4G). Moreover, the DNMT3A overexpression additionally enhanced and decreased the FZD5 promoter's transcription activity in NSCLC cells, as manifested by decreased luciferase activity of the reporter vector (Fig. 4H).

### 3.5. DNMT3A suppresses lung tumorigenesis in urethane-treated mice

To uncover the interaction that exists between DNMT3A and FZD5 as well as their roles in NSCLC development, the urethane-challenged mice were given lentiviral vectors-packaged oe-DNMT3A alone or along with oe-FZD5. Indeed, in mouse lung tissues, the administration of oe-DNMT3A substantially elevated the expression of DNMT3A (Fig. 5A). Note that decreasing the FZD5 mRNA expression was restored by oe-FZD5 (Fig. 5B). On the other hand, the tumor incidence rate in the mouse lung was reduced by DNMT3A upregulation but elevated by the restoration of FZD5 (Fig. 5C). The number of tumor nodules (Fig. 5D-E) and the degree of tumor infiltration (Fig. 5F) showed similar trends, with oe-DNMT3A reduction in the quantity of tumor nodules as well as elevation in the degree of tumor infiltration upon overexpression of FZD5. IHC assay also showed that oe-DNMT3A decreased positive staining for FZD5 and PCNA in mouse lung tissue, whereas overexpression of FZD5 increased positive staining for PCNA (Fig. 5G-H).

### 3.6. DNMT3A and FZD5 mediates malignant phenotype of NSCLC cells

Overexpression of DNMT3A and FZD5 was administered into the NCI-H1299 as well as Calu-3 cells. RT-qPCR and WB analysis successfully restored FZD5 mRNA including protein levels in both cell lines (see Fig. 6A-B). Here, the CCK-8 assay as well as the colony formation assay demonstrated that DNMT3A silencing substantially minimized the ability of cells to proliferate and form colonies, but that FZD5 upregulation prevented this outcome (see Fig. 6C-D). The outcomes pertaining to the Transwell and wound healing assays indicated that oe-DNMT3A inhibited the migration as well as invasiveness of the two cell lines. However, this suppression could be reversed by additional FZD5 upregulation.

## 4. Discussion

Characteristics of cancer cells encompass both genome-wide hypomethylation and the CpG island hypermethylation linked to developmental regulators as well as tumor suppressor genes [17]. The authors of the research found that DNMT3A had an abnormally low expression pattern in NSCLC. This leads to decreased DNA methylation level at the FZD5 promoter and the consequent gene overexpression, leading to increased lung tumorigenesis in mice and increased malignant phenotype of NSCLC cell lines.

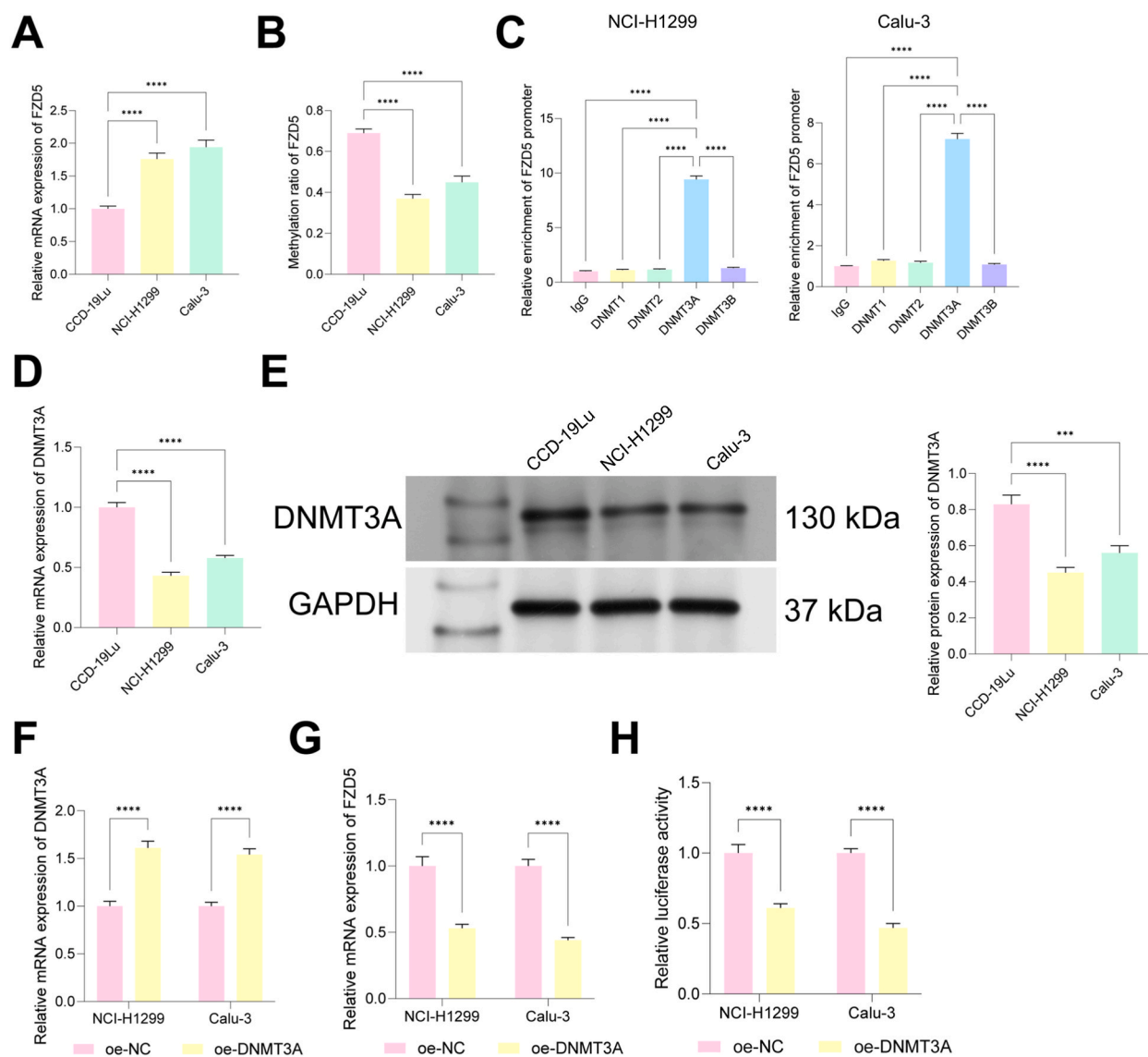


**Fig. 4.** DNMT3A promotes methylation of the FZD5 promoter. **A**, Expression of FZD5 in normal CCD-19Lu cells and NSCLC cell lines (NCI-H1299 and Calu-3) examined by RT-qPCR ( $n = 3$ ); **B**, DNA methylation level in CCD-19Lu cells and NSCLC cell lines (NCI-H1299 and Calu-3) examined by qMSP analysis ( $n = 3$ ); **C**, binding relationship between DNMT1/DNMT2/DNMT3A/DNMT3B) and FZD5 promoter in NCI-H1299 and Calu-3 cells examined by ChIP-qPCR assay ( $n = 3$ ); **D-E**, mRNA (**E**) and protein (**F**) levels of DNMT3A in CCD-19Lu cells and NSCLC cell lines (NCI-H1299 and Calu-3) determined by RT-qPCR and WB analysis, respectively ( $n = 3$ ); **F-G**, mRNA expression of DNMT3A (**F**) and FZD5 (**G**) in NCI-H1299 and Calu-3 cells after oe-DNMT3A administration determined by RT-qPCR ( $n = 3$ ); **H**, transcription activity of FZD5 promoter in NCI-H1299 and Calu-3 cells examined by luciferase assay. Differences are compared by the one-way or two-way ANOVA. \* $p < 0.05$ .

This particular study's meticulous bioinformatics analyses show that FZD5 is significantly expressed in LUAD and LUSC samples as well as is associated with a poor patient prognosis. The G protein-coupled receptors are the FZD proteins. While the intracellular C-terminus binds the PDZ domain of Dishevelled (Dvl) as well as interacts with G proteins, the extracellular N-terminus has a cysteine-rich domain that allows FZDs to bind Wnt ligands [22]. Wnt binds to FZD and, along with the co-receptor LRP5/6, initiates the formation of a ternary signaling complex. Intracellular components, for example, GSK3, CK1, APC, Axin, as well as Dvl are recruited by this complex. Moreover, the activation of Wnt target genes is the consequence of the transcriptional co-activator  $\beta$ -catenin's accumulation, which is effectively inhibited by this process [23]. Structural examinations indicate that the linker region exhibits flexibility, potentially differing across various FZDs [23,24]. It has also been reported that the FZD proteins are important in malignancies in humans. As an instance, FZD4, FZD7, as well as FZD10 have been found to be promoters of the epithelial-mesenchymal transition via the  $\beta$ -catenin pathway in breast, liver, as well as prostate cancer [25–27]. More importantly, FZD5 has been specified as a major factor supporting the establishment pertaining to a particular subtype of pancreatic ductal adenocarcinoma [8]. Knockdown of FZD5 and

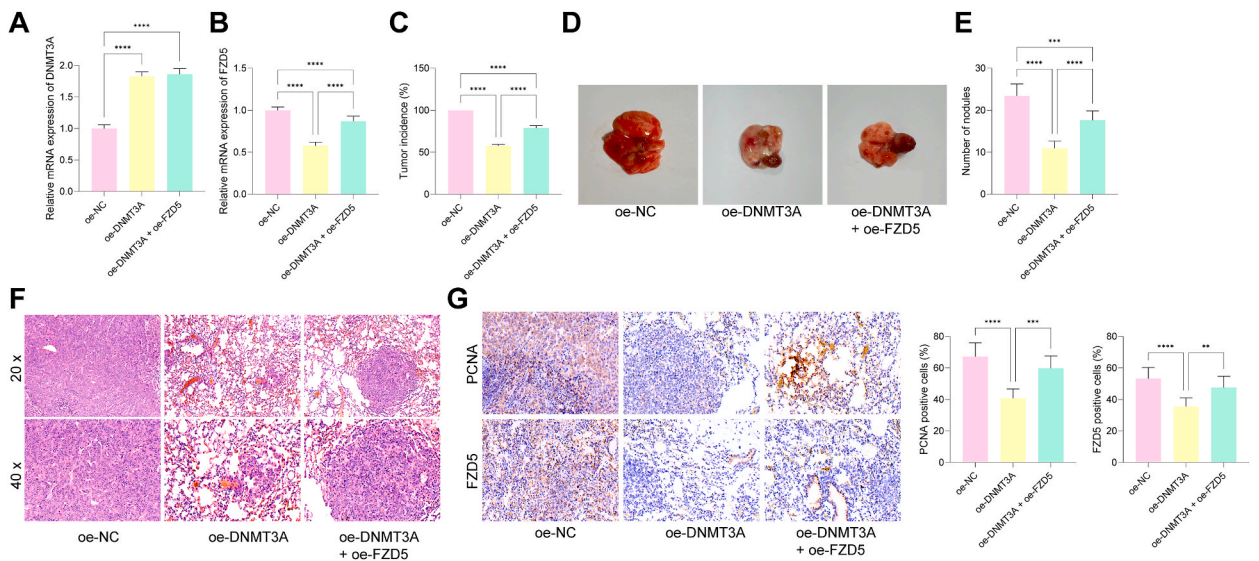


**Fig. 5.** DNMT3A suppresses lung tumorigenesis in urethane-treated mice. C57BL/6 mice were challenged with urethane to induce lung tumorigenesis, followed by tail vein injection of lentiviral vectors-carried oe-DNMT3A/oe-NC and oe-FZD5. A-B, mRNA expression of DNMT3A (A) and FZD5 (B) in the mouse lung tissues examined by RT-qPCR (n = 8); C, tumorigenesis rate in the mouse lung (n = 8); D, representative images of the mouse lung in each group; E, number of tumor nodules in the mouse lung (n = 8); F, pathological changes in the mouse lung examined by HE staining; G, expression of FZD5 and PCNA in the mouse lung tissues examined by the IHC assay (n = 8). Differences are compared by the one-way ANOVA. \**p* < 0.05.

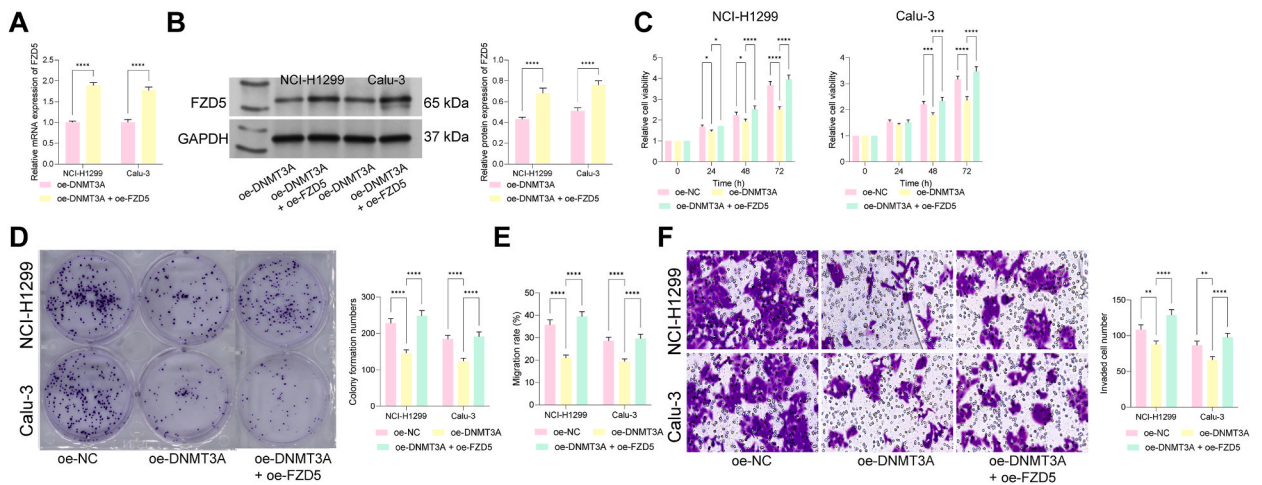


**Fig. 6.** FZD5 silencing alleviates malignant properties of NSCLC cells *in vitro*. sh-FZD5 was administered into the NCI-H1299 and Calu-3 cell lines A-B, mRNA (A) and protein (B) levels of FZD5 in cells determined by RT-qPCR and WB analysis, respectively (n = 3); C-D, proliferation (C) and colony formation (D) assay of the NCI-H1299 and Calu-3 cells determined by CCK-8 and colony formation assays, respectively (n = 3); E-F, migration (E) and invasion (F) of NCI-H1299 and Calu-3 cells analyzed by wound healing and Transwell assays. Differences are compared by the two-way ANOVA. \**p* < 0.05.

Dvl3 has been found to disrupt WNT5A-mediated activation of RHOA, consequently limiting migration of Hodgkin lymphoma cells [28]. Additionally, by initiating a signaling associated with DNA damage repair, FZD5 has been established to induce chemoresistance in triple-negative breast cancer [29]. However, an opposite role of FZD5 has been reported in gastric cancer, where it functions as a suppressor for epithelial-mesenchymal transition and correlates longer survival of patients [22]. In lung alveoli, FZD5 is specifically needed for the activity of alveolar epithelial stem cells [30]. Here in this study, complementing bioinformatics predictions, in comparison to non-tumor cells, we discovered that the FZD5 expression was lower in two NSCLC cell lines. Moreover, the NSCLC cells' migration, invasiveness, as well as proliferation were all decreased by the FZD5 silencing. More importantly, knockdown of FZD5 was found to reduce the tumorigenesis in the lung of urethane-challenged mice. These findings fill the gap of the unknown role of FZD5 in lung tumorigenesis.

Subsequent qMSP analysis illustrated that the methylation level of FZD5 was substantially reduced in lung cancer cells. This might explain the aberrant high expression pattern of FZD5 in NSCLC. Among the common DNMTs, we found that it was DNMT3A that exhibited strong binding relationship with FZD5 promoter. In a previous study by Husni et al., DNMT3a expression in LUAD samples has been correlated with a histologically non-invasive type as well as a favorable prognosis, while lacking DNMT3a was thought to promote tumor progression [31]. Plus, within a small cell lung cancer mouse model orthotopically transplanted lung organoid, forced DNMT3A expression has been discovered to restrain metastasis small cell lung cancer by suppressing the MEIS/HOX genes that promote metastasis [32]. Accordingly, we discovered in this investigation that the NSCLC cells had low levels of DNMT3A expression, and its upregulation suppressed malignant behavior of the cancer cells. Moreover, by using urethane-induced lung cancer models which is more akin to the natural course of the disease in humans, we found that the DNMT3A overexpression reduced tumorigenesis rate of primary lung tumor in mice, which was, however, rescued by the FZD5 overexpression.

This study concludes by showing that the DNMT3A low expression in NSCLC allows the transcription activation of FZD5, which leads to increased malignant phenotype of cancer cells *in vitro* and increased tumorigenesis rate of primary lung tumor in mice. However, there remain limitations in the present study. First, the Wnt ligand which interact with FZD5 and the specific downstream effector genes involved in the FZD5-mediated events remain unclear. Meanwhile, the clinical translational value pertaining to this research may be diminished by the absence of clinical samples. This study may shed new lights in this field that FZD5 may be regarded as a possible target for therapy pertaining to the management of NSCLC.

### Data availability statement

The article and supplementary materials contain the original contributions made during the research process; for additional information, please contact the corresponding author.

### Ethics approval

The procedures were acknowledged by the Fudan University Ethics Committee at Minhang Hospital (Approval number: 2023-MHFY36JZS) and adhered to the academy's guidelines for animal research.

### CRedit authorship contribution statement

**Jiqiao Shen:** Writing – original draft. **Jinchen Su:** Formal analysis. **Xiangling Chu:** Validation. **Xin Yu:** Validation. **Xiwen Gao:** Writing – review & editing.

### Declaration of competing interest

The authors declare that they have no known competing financial interests or personal relationships that could have appeared to influence the work reported in this paper.

### Appendix A. Supplementary data

Supplementary data to this article can be found online at <https://doi.org/10.1016/j.heliyon.2024.e29733>.

### References

- [1] H. Sung, et al., Global cancer statistics 2020: GLOBOCAN estimates of incidence and mortality worldwide for 36 cancers in 185 countries, *CA A Cancer J. Clin.* 71 (3) (2021) 209–249.
- [2] Y.H. Luo, et al., Lung cancer in Republic of China, *J. Thorac. Oncol.* 16 (4) (2021) 519–527.
- [3] Z. Ma, et al., Lung cancer risk score for ever and never smokers in China, *Cancer Commun.* 43 (8) (2023) 877–895.
- [4] A. Leiter, R.R. Veluswamy, J.P. Wisnivesky, The global burden of lung cancer: current status and future trends, *Nat. Rev. Clin. Oncol.* 20 (9) (2023) 624–639.
- [5] S. Jonna, D.S. Subramaniam, Molecular diagnostics and targeted therapies in non-small cell lung cancer (NSCLC): an update, *Discov. Med.* 27 (148) (2019) 167–170.
- [6] S.R. Broderick, Adjuvant and neoadjuvant immunotherapy in non-small cell lung cancer, *Thorac. Surg. Clin.* 30 (2) (2020) 215–220.
- [7] N. Duma, R. Santana-Davila, J.R. Molina, Non-small cell lung cancer: epidemiology, screening, diagnosis, and treatment, *Mayo Clin. Proc.* 94 (8) (2019) 1623–1640.
- [8] S. Zheng, et al., Aberrant cholesterol metabolism and wnt/ $\beta$ -catenin signaling coalesce via Frizzled5 in supporting cancer growth, *Adv. Sci.* 9 (28) (2022) e2200750.
- [9] B.T. MacDonald, X. He, Frizzled and LRP5/6 receptors for Wnt/ $\beta$ -catenin signaling, *Cold Spring Harbor Perspect. Biol.* 4 (12) (2012).
- [10] H.C. Huang, P.S. Klein, The Frizzled family: receptors for multiple signal transduction pathways, *Genome Biol.* 5 (7) (2004) 234.
- [11] P.N. Le, J.D. McDermott, A. Jimeno, Targeting the Wnt pathway in human cancers: therapeutic targeting with a focus on OMP-54F28, *Pharmacol. Ther.* 146 (2015) 1–11.
- [12] M.L. Bats, et al., Wnt/frizzled signaling in endothelium: a major player in blood-retinal- and blood-brain-barrier integrity, *Cold Spring. Harb. Perspect. Med.* 12 (4) (2022).
- [13] D.J. Stewart, Wnt signaling pathway in non-small cell lung cancer, *J. Natl. Cancer Inst.* 106 (1) (2014) djt356.
- [14] L.D. Moore, T. Le, G. Fan, DNA methylation and its basic function, *Neuropsychopharmacology* 38 (1) (2013) 23–38.

- [15] M. Kulis, M. Esteller, DNA methylation and cancer, *Adv. Genet.* 70 (2010) 27–56.
- [16] J. Duan, et al., DNA methylation in pulmonary fibrosis and lung cancer, *Exp. Rev. Respir. Med.* 16 (5) (2022) 519–528.
- [17] A. Nishiyama, M. Nakanishi, Navigating the DNA methylation landscape of cancer, *Trends Genet.* 37 (11) (2021) 1012–1027.
- [18] P. Li, et al., Liquid biopsies based on DNA methylation as biomarkers for the detection and prognosis of lung cancer, *Clin. Epigenet.* 14 (1) (2022) 118.
- [19] X. Gu, et al., Development and validation of a DNA methylation-related classifier of circulating tumour cells to predict prognosis and to provide a therapeutic strategy in lung adenocarcinoma, *Int. J. Biol. Sci.* 18 (13) (2022) 4984–5000.
- [20] D. Wu, et al., TANC1 methylation as a novel biomarker for the diagnosis of patients with anti-tuberculosis drug-induced liver injury, *Sci. Rep.* 11 (1) (2021) 17423.
- [21] Y. Pan, et al., DNA methylation profiles in cancer diagnosis and therapeutics, *Clin. Exp. Med.* 18 (1) (2018) 1–14.
- [22] D. Dong, et al., FZD5 prevents epithelial-mesenchymal transition in gastric cancer, *Cell Commun. Signal.* 19 (1) (2021) 21.
- [23] N. Tsutsumi, et al., Structure of human Frizzled5 by fiducial-assisted cryo-EM supports a heterodimeric mechanism of canonical Wnt signaling, *Elife* 9 (2020).
- [24] S. Yang, et al., Crystal structure of the Frizzled 4 receptor in a ligand-free state, *Nature* 560 (7720) (2018) 666–670.
- [25] S. Gupta, et al., FZD4 as a mediator of ERG oncogene-induced WNT signaling and epithelial-to-mesenchymal transition in human prostate cancer cells, *Cancer Res.* 70 (17) (2010) 6735–6745.
- [26] S.B. Nambotin, et al., Functional consequences of WNT3/Frizzled7-mediated signaling in non-transformed hepatic cells, *Oncogenesis* 1 (10) (2012) e31.
- [27] C. Gong, et al., BRMS1L suppresses breast cancer metastasis by inducing epigenetic silence of FZD10, *Nat. Commun.* 5 (2014) 5406.
- [28] F. Linke, et al., WNT5A: a motility-promoting factor in Hodgkin lymphoma, *Oncogene* 36 (1) (2017) 13–23.
- [29] Y. Sun, et al., FZD5 contributes to TNBC proliferation, DNA damage repair and stemness, *Cell Death Dis.* 11 (12) (2020) 1060.
- [30] A.N. Nabhan, et al., Targeted alveolar regeneration with Frizzled-specific agonists, *Cell* 186 (14) (2023), 2995-3012.e15.
- [31] R.E. Husni, et al., DNMT3a expression pattern and its prognostic value in lung adenocarcinoma, *Lung Cancer* 97 (2016) 59–65.
- [32] F. Na, et al., KMT2C deficiency promotes small cell lung cancer metastasis through DNMT3A-mediated epigenetic reprogramming, *Nat. Can. (Ott.)* 3 (6) (2022) 753–767.